Rates, timing, and mechanisms of rainfall interception loss in a coastal redwood forest

Leslie M. Reid *, Jack Lewis

Redwood Sciences Laboratory, US Forest Service Pacific Southwest Research Station, 1700 Bayview Drive, Arcata, CA 95519, USA

S U M M A R Y

Rainfall, throughfall, and stemflow were monitored at 5-min intervals for 3 years in a 120-year-old forest dominated by redwood (*Sequoia sempervirens*) and Douglas-fir (*Pseudotsuga menziesii*) at the Caspar Creek Experimental Watersheds, located in northwest California, USA. About 2.5% of annual rainfall reaches the ground as stemflow at the site, while 22.4% is stored on foliage and stems and evaporates before reaching the ground. Comparison of the timing of rainfall and throughfall indicates that about 46% of the interception loss occurs through post-storm evaporation from foliage and 54% is either evaporated during the storm or enters long-term storage in bark. Until bark storage capacity is saturated, the proportion of rainfall diverted to bark storage would be relatively constant across the range of rainfall intensities encountered, reflecting primarily the proportional incidence of rainfall on surfaces contributing to bark storage. In any case, loss rates remain high—over 15%—even during the highest-intensity storms monitored. Clear-cut logging in the area would increase effective annual rainfall by 20–30% due to reduction of interception loss, and most of the increase would occur during large storms, thus potentially influencing peakflows and hillslope pore-pressures during geomorphically significant events.

Published by Elsevier B.V.

Introduction and background

Foliage in temperate forests is widely reported to intercept and evaporate 10–40% of annual rainfall (e.g., Maidment, 1993), but questions remain concerning the relative importance of various mechanisms for evaporative loss. We monitored rainfall and throughfall in a coastal redwood forest during 250 rain events to assess the importance of the process in this environment, describe the timing of rainfall interception during storms, evaluate its seasonal relevance to the water balance, and assess its potential implications for forest management in the area.

Improved technology and understanding have allowed increasingly detailed study of interception over the past 100 years, and recent studies have focused on such aspects as quantifying canopy water storage (Vrugt et al., 2003), evaluating temporal and spatial variability of throughfall (Keim et al., 2005), and assessing the influence of canopy structure on interception rates (Pypker et al., 2005). Studies have consistently shown that the proportion of storm rainfall intercepted tends to be highest for small storms on dry canopies, during which most rainfall encountering foliage is held onto the foliage by surface tension. This component does not drain under gravity and so is available for evaporation after rainfall ceases. Rainfall continues to be lost to interception even after non-draining storage is filled, however, in part because water continues to evaporate during rainfall if, as is usually the case, air is not saturated during the storm.

Several models have been constructed to predict rates of interception loss as a function of atmospheric conditions and forest characteristics (e.g., Gash, 1979; Liu, 1997), and such models have been applied successfully in a variety of settings (e.g., Link et al., 2004; Bryant et al., 2005). However, Murakami (2006) points out that because of empirical parameterization used in the models, a model's success does not necessarily indicate that the process is well understood, and he notes, in particular, that explanations for the dependence of evaporation rate on rainfall intensity are theoretically unsatisfactory. Klaassen et al. (1998) suggest that models severely underestimate storage volume and, consequently, underestimate the relative importance of post-storm evaporation, while others, such as Crockford and Richardson (1990b), hold that in-storm evaporation is the more important mechanism. The relative importance of these processes undoubtedly varies by storm, forest type, and climatic setting, so an analytical approach that distinguishes between these components would contribute to refinement of predictive models. We examine throughfall measurements recorded at a fine temporal scale to explore the relative importance of within-storm losses and post-storm evaporation at a study site in northwest California, USA.

* Corresponding author. Tel.: +1 707 825 2933; fax: +1 707 825 2901.
E-mail address: lreid@fs.fed.us (L.M. Reid).

Study site

The 4.7-km^2 North Fork Caspar Creek watershed (N39°21′ W123°44′) is located 10 km south of Fort Bragg, California, USA, and 6 km from the Pacific Ocean at an elevation of 85–320 m. Annual rainfall between 1978 and 2001 averaged 1285 mm, with 95% falling during October–April, mostly during relatively long-duration, low-intensity frontal storms. Snow is infrequent, and temperatures are moderate through the year, ranging from an average of 7 °C in December to 16 °C in July. Valleys in the area are frequently inundated by coastal fog during summer. Average annual runoff from the North Fork for 1978–2001 was 626 mm, accounting for about half of annual rainfall.

The original forest in the North Fork watershed was cut in the late 1800s, and about 50% of the watershed was logged again in 1985–1991 during an experiment designed to measure the hydrologic and erosional effects of clearcut logging. Two 1-ha plots were established in second-growth forest to monitor rates of rainfall interception. The Iverson plot (IVE) is located at an elevation of 220 m on a southeast-facing slope, and the Munn plot (MUN) is 1.5 km east at 270 m on a north-facing slope (Table 1). Both stands are dominated by 120-year-old redwood (*Sequoia sempervirens*) and Douglas-fir (*Pseudotsuga menziesii*), but the IVE stand has a slightly lower basal area of trees and a less uniform canopy than the MUN stand, and, unlike MUN, has a patchy but well-developed sub-canopy of hardwoods and young conifers. One corner of each study plot is within 20 m of a clearcut unit that was logged in 1989 (MUN) or 1991 (IVE), allowing placement of rain gauges in clearings near each plot.

Methods

Terminology has not been consistently applied in past studies of rainfall interception. Some researchers use "interception" to mean the process of evaporation of water trapped on foliage, while others apply the term to the process of trapping of the water, whether or not it is eventually evaporated. In this paper, we use "rainfall interception" in a general sense to indicate the difference between rainfall and throughfall in a specified time interval; "intercepted" rain may eventually evaporate, flow to the ground as stemflow, or drip to the ground during a subsequent time interval. We reserve the term "interception loss" to refer to the component of intercepted water that does not eventually reach the ground through stemflow or drip. "Throughfall" refers to the component of rainfall that either does not encounter foliage or that drips to the ground after being temporarily stored on foliage (i.e., that com-

Fig. 1. Throughfall collector (1.2 m × 1.2 m) and plastic storage barrel, which is suspended from a load cell.

ponent collected in rain gauges under the forest canopy), and "stemflow" is the component that is diverted to tree boles and eventually flows to the ground.

To evaluate throughfall, six 1.22 × 1.22 m throughfall collectors were distributed randomly across each plot. Each collector consisted of a plywood sheet surrounded by 14-cm walls (Fig. 1); surfaces were sealed with enamel paint. Each collector was installed at a 25° angle to facilitate drainage, producing a projected area of 1.35 m^2. Collected water flowed through a screened outlet into a polyethylene tube, which directed flow into a 150-l plastic barrel suspended from a load cell. Load cell readings were recorded by a data logger at 5-min intervals. At each plot, a seventh collector was located in the adjacent clearcut to serve as a control, along with a standard 20.3-cm-diameter tipping-bucket rain gauge mounted at ground level, an anemometer, and a thermistor. Data from these instruments were also recorded at 5-min intervals. The study is based on monitoring results from 5 December 1998 to 27 May 2001 at IVE and from 1 December 1998 to 8 November 1999 at MUN.

Load cells were calibrated once each season, and, in computation of throughfall, changes in calibration coefficients were assumed to progress linearly with time. Load cell "noise" became a problem as the study progressed. These signal fluctuations were evaluated by plotting apparent throughfall during rainless periods. Periods for which anomalous mean daily fluctuations exceeded 1 mm were removed from the data, resulting in the loss of data from the IVE collector I6 beginning in February 1999, all collectors at MUN as of November 1999, and the I1 collector in April 2000. A few periods of barrel leakage were corrected using the leakage rate measured after rainfall ended. Data from each standard rain gauge were adjusted based on measurements of total volume collected in that gauge, generally on an annual basis. With the exception of a 16% correction required for a 28-day period encompassing 3 events near the end of the study, the maximum adjustment was 2.2%.

Missing data resulting from equipment maintenance, overtopped barrels, or plugged water lines were later replaced using imputation models based on 2-h, non-zero rainfall totals, considering complete cases only (Table 2). Linear regression, weighted by the inverse of rainfall, employed data from up to three of the other gauges as predictors. After its load cell failed, a lengthy record from I1 was imputed because it had the highest throughfall of the IVE collectors and removing it could have biased the results. Comparison of results before and after April 2000 indicates that conclusions would not have changed had the study terminated when collector I1 was lost. The additional year of data—incorporating imputed estimates for collector I1—was included to explore year-

Table 1
Characteristics of the IVE and MUN plots. Subtotals are italicized.

	IVE	MUN
Period of record	12/5/1998-5/27/2001	12/1/1998-11/8/1999
Aspect	South-east	North
Plot area (ha)	1.0	1.0
Number of events	250	78
Elevation (m)	220	270
Stand composition (stems)[a]		
Redwood	*341*	*341*
Douglas-fir and other conifer	*108*	*119*
Tanoak and other hardwood	*89*	*15*
Total	538	475
Stand basal area (m^{2}ha^{-1})		
Redwood	*61*	*59*
Douglas-fir and other conifer	*31*	*49*
Tanoak and other hardwood	*5.5*	*0.9*
Total	97	108

[a] Stems of diameter greater than 13 cm were inventoried.

Table 2
Throughfall and rainfall measurements at IVE and MUN plots. Gauges I1-7 and M1-7 are plywood platform collectors.

Gauge	Percent cover	Percent imputed	Precipitation (mm) in hydrologic year:		
			HY99	HY00	HY01
Iverson plot					
I1	79	46.6[a]	924	1043	615[a]
I2	73	1.2	752	807	438
I3	75	1.6	829	887	564
I4	90	2.0	846	938	542
I5	100	0.1	518	537	293
I7: control	0	4.1	987	1131	685
I tipping bucket	0	2.0	1024	1213	726
Mean % throughfall[b]			78.3	74.5	71.6
Munn plot					
M1	76	8.4	838		
M2	74	2.9	800		
M3	74	8.3	817		
M4	84	0.1	779		
M5	69	7.8	876		
M6	92	0.2	890		
M7: control	0	2.2	1043		
M tipping bucket	0	0.0	1086		
Mean % throughfall[b]			79.9		

[a] Data imputed for I1 during HY01.
[b] Calculated relative to control collectors, I7 or M7.

to-year variation on the plot. The 2 months of valid data from collector I6 showed its throughfall to be about average, so its record would have reduced the variance of the results but would not have affected mean values.

Comparison of rainfall estimates from the control collectors to those of the adjacent standard gauges allows evaluation of trap efficiency for the plywood collectors. The control collectors at IVE and MUN recorded annual totals 4–7% lower than those recorded by standard gauges (Table 2), suggesting that processes such as splash and evaporation from the collectors may decrease their trap efficiency. Wind-driven rain also could be significantly under- or overestimated on an inclined collector, but the similarity of the IVE and MUN comparisons suggests that orientation of the collector is not a primary cause. Proportional loss tends to be greater for small storms, suggesting that evaporation is more influential than splash. The disproportionate loss during small storms introduces a potential bias because those collectors demonstrating interception loss—and therefore effectively experiencing smaller storms than the control collector—would tend to show higher loss rates than would actually be present. The magnitude of this bias was estimated by using the relationship between measurements at the IVE rain gauge and at the control collector to calculate throughfall with and without a correction, and the influence was found to be negligible.

For calculations of interception loss described below, data from forested throughfall collectors are compared to data from control collectors on the assumption that trap efficiency is the same for collectors inside and outside the forest stand. If trap efficiency is actually lower in the clearing, as would occur if wind-driven rain is undersampled or if evaporation rates are higher in the clearing, then the standard gauge may provide a better estimate of above-canopy rainfall, and our estimates of interception loss may be low by as much as 3% of annual rainfall.

To estimate stemflow, 24 trees (12 redwoods, 8 Douglas-firs, and 4 tanoaks [*Lithocarpus densiflora*]) at IVE were selected randomly from strata defined by species and diameter. A groove was cut into the bark of each tree, and each was fitted with a rubber collar that channeled flow into one or more plastic containers. Between 2 December 1999 and 20 April 2001, water depth in each container was measured with a dipstick at 2-day to 4-week intervals through the wet season. Methods and results are described in more detail by Lewis (2003). Flows from six of the trees, including three redwoods, two Douglas-firs, and a tanoak, were routed through tipping-bucket gauges to record stemflow timing. Records from these gauges were adjusted to match volumes accumulated in the containers.

Results

Throughfall

The 11 collectors operating between 5 December 1998 and 7 November 1999 show an average throughfall of 79 ± 7% (95% CI) over the 11-month period, with IVE showing a slightly lower throughfall (78%) than MUN (80%). Variance between collectors at IVE is considerably greater (standard deviation of 16%) than at MUN (s.d. 4%), probably reflecting the denser sub-canopy and less uniform canopy at IVE. Point counts of the central portions of photographs taken upward from the centers of collectors show a mean foliage cover of 79% (s.d. 14%) at IVE and 78% (s.d. 8%) at MUN. Although the plot with the greatest variation in cover has the highest variability in throughfall, throughfall measured at specific collectors is not correlated with foliage cover directly overhead. The lack of correlation may reflect both non-vertical trajectories of rain and its local redistribution by foliage.

Mean annual percentage of throughfall varied over the 3-year measurement period at IVE (Table 2), as did the distribution of storms, so throughfall was reevaluated by event to determine whether differences in storm character contributed to interannual variation. Examination of 5-min-resolution throughfall records suggests that 98% of canopy drip has occurred by 3 h after the last rain was recorded at the standard rain gauge, so individual rainfall events are defined for these sites as periods of rain separated by at least 3 h of no rain at the standard gauge. The 2.5-year monitoring period at IVE produced 250 events, while 78 were recorded during 11 months at MUN. Four events having significant hail or snowfall were excluded from the analysis.

At each plot, throughfall is well approximated by a segmented linear function of event rainfall constrained to pass through the origin. For IVE (Fig. 2a):

for $P_{c3} \geqslant 4.68$ mm $\quad T = -1.37 + 0.827 P_{c3} \quad n = 106 \qquad$ (1a)

for $P_{c3} < 4.68$ mm $\quad T = 0.533 P_{c3} \quad n = 140 \qquad$ (1b)

where T is mean throughfall for the 5 collectors (mm) and P_{c3} is gross rainfall (mm) measured at the control collector for events occurring between non-rain periods of 3 h or more. Equivalent relations derived for MUN are similar (Fig. 2b):

for $P_{c3} \geqslant 3.11$ mm $\quad T = -1.56 + 0.870 P_{c3} \quad n = 40 \qquad$ (2a)

for $P_{c3} < 3.11$ mm $\quad T = 0.369 P_{c3} \quad n = 36 \qquad$ (2b)

Annual totals estimated using Eqs. (1) for IVE are within 2% of the values measured for each year (78% observed vs. 77% predicted for HY99, 74% vs. 75% for HY00, and 72% vs. 74% for HY01, where a Hydrologic Year (HY) is defined to begin on 1 August of the preceding calendar year), suggesting that differences in event size may explain much of the interannual variation in throughfall. Overall, about 25% of the rainfall at IVE is diverted by the canopy to either evaporate or reappear as stemflow.

Maximum possible free throughfall—that not influenced by foliage—is estimated as 100% minus the percent foliage cover, or 21% at IVE and 22% at MUN. This estimate assumes rain falls vertically, which is generally not the case. A second estimate is derived from throughfall rates measured during the first 5 min of storms that begin with high-intensity bursts of greater than 6 mm h^{-1} at the control collector. Initial 5-min throughfall rates for nine such storms at IVE and three at MUN suggest that free throughfall is approximately 8 ± 3% (95% CI) of total rainfall.

Stemflow

The volume of stemflow accumulated over 2-day to 4-week periods was measured from 24 trees at IVE (Steinbuck, 2002). Plot totals were computed from measured volumes for each species and measurement period by applying a general ratio estimator (Särndal et al., 1992) to the stratified sampling design (Lewis, 2003). In essence, stemflow and its variance were modeled as power functions of diameter to permit estimation of stemflow volume for each redwood, Douglas-fir, and tanoak in the plot. Stemflow from the three monitored species was estimated as 2.7 ± 0.5% (95% CI) of rainfall for the HY00 monitoring period and 2.2 ± 0.5% for HY01. Lewis (2003) presents relations between annual stemflow and stem diameter for the three species (Eq. (16) and Table 5 in Lewis, 2003). Twelve trees of unmonitored species were also present among the 538 trees on the IVE plot. Application of the relevant equation for the most similar monitored species increases the estimated stemflow by about 0.08% of annual rainfall.
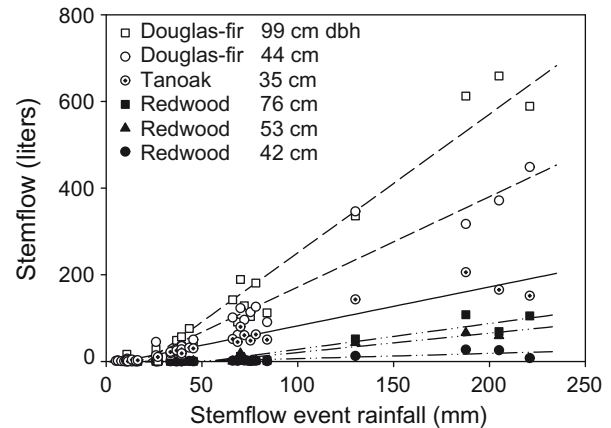

Fig. 3. Stemflow for six instrumented trees as a function of stemflow event size.

Finer resolution data from the six trees instrumented with tipping-bucket gauges now permit stemflow to be evaluated by event. These data demonstrate that stemflow may continue to drain for up to 48 h after cessation of rainfall. It would thus be difficult to accurately partition stemflow into the throughfall events defined above, so stemflow events are defined for this site as periods of rain separated by at least 48 h without rain. Event-based data for each tree show a linear increase in stemflow volumes with increasing rainfall (Fig. 3). Within a species, the similarity of *x*-intercepts suggests the threshold rainfall for generating stemflow is relatively consistent. Stemflow events thus fall into four categories: events of <8.5 mm generate no stemflow; those of 8.5–19.5 mm produce stemflow only from tanoaks; of 19.5–51.2 mm, from tanoaks and Douglas-fir; and of >51.2 mm, from all species.

Lewis' equations estimate stemflow for specific stemflow monitoring periods at IVE, but estimates are here needed for all stemflow events of HY99 to HY01 as defined for this study. Stemflow volumes for the 22 events of hydrologic year 2001 for which stemflow was monitored were first calculated for each of the 6 continuously monitored trees to calculate each event's proportional contribution to the total stemflow for that tree. Because the relations between event stemflow volume and event rainfall are linear and intercepts are similar within a species (Fig. 3), proportional contributions are independent of tree size within a species, so proportions were then averaged by species. The plot total for each species, as provided by Lewis (2003) and modified to include the additional species present, was distributed among events by
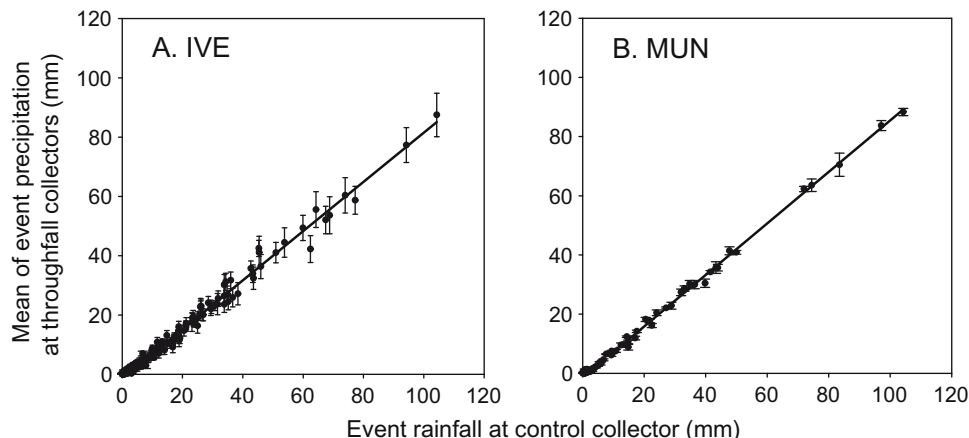

Fig. 2. Event throughfall as a function of event rainfall at (A) IVE and (B) MUN. Error bars indicate the standard error of the mean for throughfall collectors at each plot.
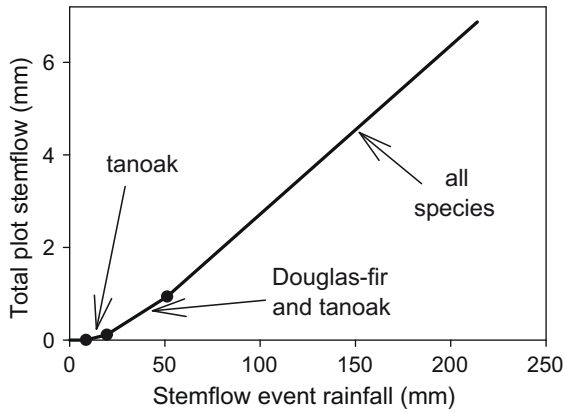
Fig. 4. Relationships between total plot stemflow and stemflow event rainfall for the IVE plot.

applying the calculated proportions. Results for each event were summed across species. These estimates of event-based total plot stemflow (S_t, mm) were used to calculate the relationship between stemflow and rainfall (P_{c48}, mm, defined on the basis of 48-h dry periods) at the IVE control collector (Fig. 4), and the result then allowed estimation of plot totals for each stemflow event during the 3-year period.

Stemflow is estimated to account for 2.7% of rainfall for HY99, 2.5% for HY00, and 2.2% for HY01. The percentage of rainfall contributing to stemflow increases slightly with event rainfall, reaching 3.3% for events equivalent to the largest measured (268 mm). Although only 17% of the trees (corresponding to 6% of the basal area) are tanoak or similar species, these account for about 38% of the annual stemflow, while the 341 redwood trees present (63% of trees and 62% of basal area) account for only 15% of the total.

Similar calculations were used to estimate stemflow on the basis of stand composition and rainfall for MUN. This site has a higher proportion of Douglas-fir than IVE and a lower proportion of hardwoods (Table 1). Stemflow for HY99 is estimated to be 2.4% of rainfall, slightly lower than the 2.7% estimated for the same period at IVE.

Storm-scale rainfall interception loss

Rainfall interception loss is estimated for each stemflow event by subtracting throughfall and stemflow from rainfall measured at the control collector. Stemflow events (defined using 48-h breaks in rainfall) often include multiple throughfall events (defined by 3-h breaks), so throughfalls measured for the component events are summed to calculate total throughfall for the stemflow events. The percentage of rainfall lost through interception at IVE decreases with event rainfall until approaching an asymptote of about 21% for events larger than 70 mm (Fig. 5). Over the measurement period, interception loss accounts for an average of 22.4% of annual rainfall at IVE (Table 3). A linear regression (weighted by the inverse of event rainfall to account for non-uniform variance)
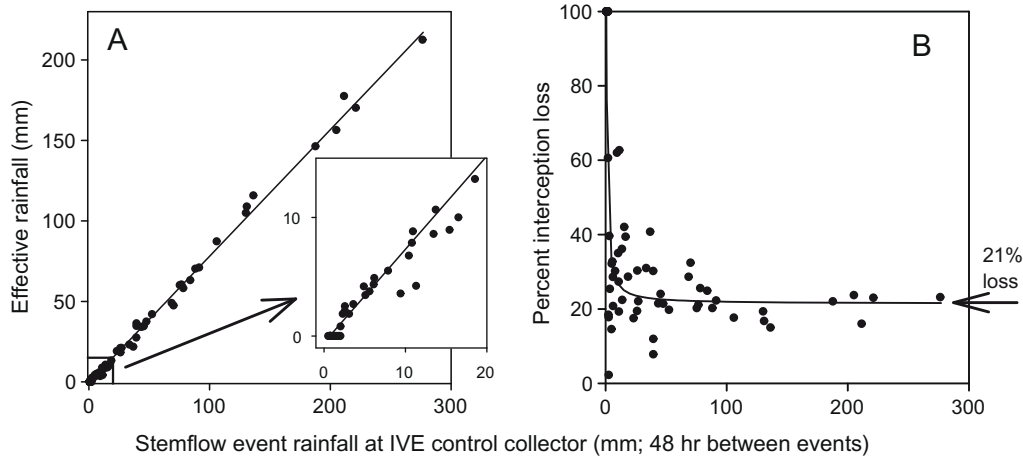

Fig. 5. (A) Effective rainfall as a function of total event rainfall measured at the IVE control collector for events defined on the basis of 48-h dry periods (inset provides detail for small events). (B) Percent interception loss as a function of event rainfall. The plotted line is calculated from Eq. (3a), and 26 events with less than 2 mm of rain produced no measurable throughfall and thus appear superimposed at 100% interception loss.

Table 3
Components of the canopy water balance associated with rainfall. Subtotals are italicized.

	MUN HY99	IVE HY99	IVE HY00	IVE HY01	IVE 3-year average
Rainfall, tipping bucket (mm)	1086	1024	1213	726	988
Percent throughfall					
Free throughfall	*9.0*	*8.0*	*8.0*	*8.0*	*8.0*
Delayed by foliage	*70.9*	*70.3*	*66.5*	*63.6*	*67.1*
Total	*79.9*	*78.3*	*74.5*	*71.6*	*75.1*
Percent stemflow	2.4	2.7	2.5	2.1	2.5
Percent evaporation					
During rain from foliage and bark; after rain from bark	*12.0*	*12.0*	*12.0*	*12.0*	*12.0*
After rain from foliage	*5.7*	*7.0*	*11.0*	*14.3*	*10.4*
Total	*17.7*	*19.0*	*23.0*	*26.3*	*22.4*

of effective rainfall at IVE (R_e, the sum of throughfall and stemflow) against gross rainfall defined by 48-h dry periods (P_{c48}, mm) for 78 events (Fig. 5a) allows effective rainfall to be estimated as:

for $P_{c48} \geqslant 0.7$ mm $R_e = -0.548 + 0.786 P_{c48}$ $r^2 = 0.99$ (3a)
for $P_{c48} < 0.7$ mm $R_e = 0$ (3b)

and interception loss is then calculated as the difference between total and effective rainfall. The influence of free throughfall, corresponding to about 8% of rainfall, was not distinguishable for storms of less than 0.7 mm due to measurement resolution. Refinement of Eqs. (3) to explicitly incorporate stemflow thresholds did not significantly improve the fit. Interception loss in the second-growth redwood forests at Caspar Creek is toward the low end of the range of 17–41% measured in other coastal coniferous forests of northwestern North America (McMinn, 1960; Spittlehouse, 1998; Patric, 1966).

Discussion

Relative importance of post-rainfall evaporation from foliage

Raindrops entering a forest canopy can meet one of several fates (Fig. 6). Drops that do not impinge on foliage hit the forest floor as free throughfall. Those that encounter foliage can (1) be retained in non-draining storage on foliage by surface tension; (2) be shattered into droplets by their impact with foliage and resume their fall; (3) be temporarily stored on foliage until they are dislodged by an incoming drop or coalesce with enough other drops to drip to the ground; or flow along the branches and stem until they either (4) are absorbed by bark or (5) flow to the ground as stemflow.

Drops that encounter foliage are delayed in their transfer to the ground, thus prolonging the duration over which evaporation can take place. At the end of the storm, the component of stored water that does not drain through gravity (paths 1 and 4; referred to as "static" storage) will either evaporate or be absorbed by the plant and evaporated later. Drops following paths 2, 3, and 5 are effectively stored over the length of time they are delayed in their transit to the ground. This storage component (termed "dynamic" storage) increases with increasing rainfall intensity, but water that survives evaporation during the delay will eventually drain. Examination of throughfall records at IVE allows quantification of transport through several of these pathways.

The timing of interception at Caspar Creek can be determined using the 5-min-resolution throughfall data by plotting the cumulative difference between rainfall and throughfall as an event progresses (e.g., Fig. 7). Plots for most storms show rapid interception rates until about 8 mm of rain have fallen (Fig. 7b); Klaassen et al. (1998) identified the same threshold rainfall in a Douglas-fir plantation in the Netherlands. After this, average interception rates (expressed per unit time) decrease and begin to fluctuate more with changes in rain intensity (Fig. 7a). If rates are expressed per unit rainfall, however, they remain relatively constant after wet-up (Fig. 7b).
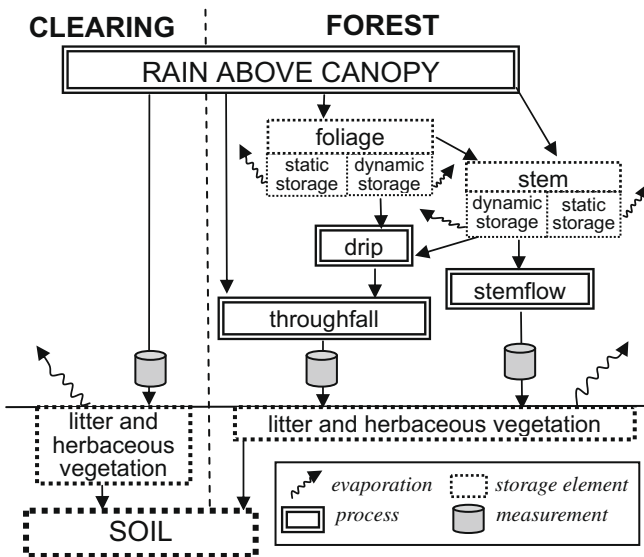

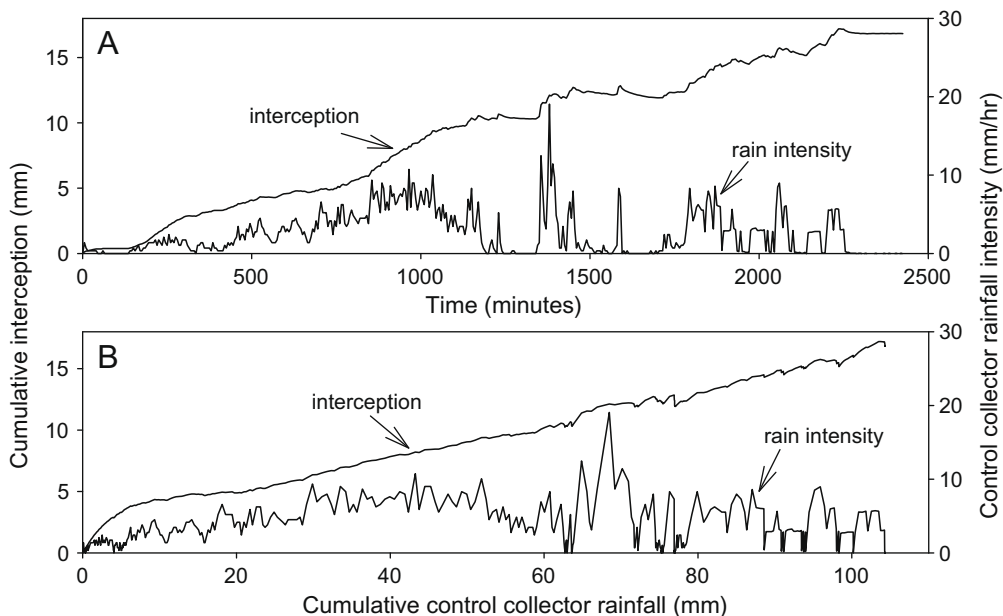**Fig. 6.** Components of the canopy water balance associated with rainfall.

Fig. 7. Cumulative interception (calculated as the difference between cumulative rainfall and cumulative throughfall) for throughfall event IVE24 (2/5/1999–2/7/1999) as a function of (A) time and (B) cumulative rain.

The initial period of rapid interception (Fig. 8) represents filling of the most accessible storage sites for water in the canopy, and this storage element provides a major source for post-storm evaporation from static foliar storage (path 1). However, processes such as in-rain evaporation that are active after the wet-up period also occur during wet-up, so to estimate the volume associated with static storage on foliage, it is necessary to first estimate the rate of interception by a canopy in which static foliar storage has been filled, which is here referred to as the "wetted retention rate" (Fig. 8).

The 250 events at IVE were screened for periods of uniform intensity after more than 9 mm of rain had fallen (criteria: rain intensity is greater than 2 mm h^{-1} and has a standard deviation of less than 30% of the mean intensity for more than 15 min). The wetted retention rate expressed per unit time (W, mm h^{-1}) is found to increase with rain intensity (P_i, mm h^{-1}) (Fig. 9a):

$$W = -0.480 + 0.242P_i \quad n = 71 \quad r^2 = 0.78 \tag{4}$$

If 3% of the rainfall after wet-up is assumed to eventually reach the ground through stemflow, approximately 1.6 mm h^{-1} is unaccounted for during 10-mm h^{-1} rain periods and 3.8 mm h^{-1} during 20-mm h^{-1} rain periods.

A replot of the data in Fig. 9a in terms of wetted retention per millimeter of rain shows high variance but no statistically significant relation to rain intensity at the 0.05 level (Fig. 9b); wetted retention accounts for an average of 15% (95% CI ±2%, s.d. 9.2%)
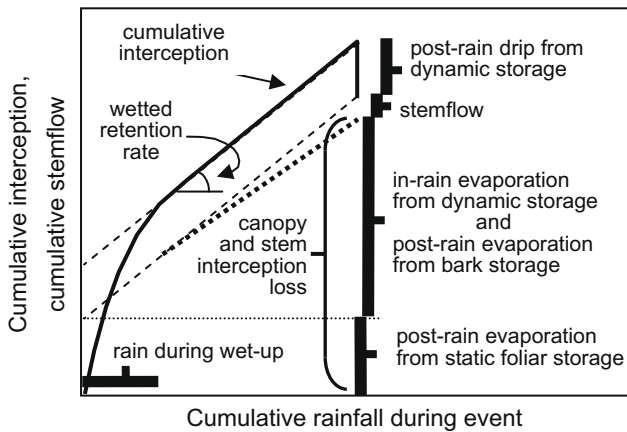
of rainfall at IVE and 14% (95% CI ±1%, s.d. 5.6%) at MUN. When average annual stemflow is subtracted, wetted retention represents an average of 12% of rainfall at both sites. Over a year, the component of rainfall accounted for by wetted retention would be equivalent to about 54% of the total interception loss at the site. The remaining 46% occurs by evaporation of a quantity of water equivalent to that intercepted during the initial wet-up phase and which cannot be accounted for by the wetted retention rate, stemflow, or post-storm drip (Fig. 8). This quantity is likely to represent the volume held in non-draining storage on foliage surfaces, and so would be roughly equivalent to the volume evaporated from foliage surfaces after rainfall ends.

Potential mechanisms for interception loss associated with wetted retention

The fate of water that continues to be intercepted after the wet-up period—that diverted to wetted retention—is more perplexing, and the relatively constant wetted retention rate of 12% of rainfall across a range of rainfall intensities is particularly puzzling. Two mechanisms have been proposed in the past to explain continued interception after wet-up: (1) evaporation of stored water during the storm (e.g., Crockford and Richardson, 1990b), and (2) enhanced evaporation of droplets formed when raindrops hit foliage (e.g., Murakami, 2006). A third potential mechanism is introduced here: (3) diversion to bark storage. We propose in this section that the first and third of these mechanisms are the dominant influences explaining the observed interception loss associated with wetted retention in the Caspar Creek forest.

In-rain evaporation of stored water

The influence of foliar storage on interception loss can be estimated by considering the increased surface area that foliage provides for evaporation of temporarily stored water. Daily open-pan evaporation was measured for 10 years at Ferndale, California, located 6 km from the coast 90 km north of Caspar Creek in an area with similar climate (NOAA, unpublished data for 3/17/63–9/30/73 at station 043030, Ferndale 2 NW). Regression of daily evaporation against number of hours without rain in the day suggests that mid-winter in-rain evaporation (estimated as the y-intercept of the regression) averages about 0.006 mm^3 h^{-1} per mm^2 of wetted surface (95% CI: 0.0005–0.012 mm h^{-1}). Evaporation rates are higher in spring and fall and highest in summer. While the uncertainty of this estimate is high, the estimate is useful for indicating the likely order of magnitude for the rate.

Fig. 8. Illustration of terms used in evaluations of interception components as they apply to plots of cumulative interception.
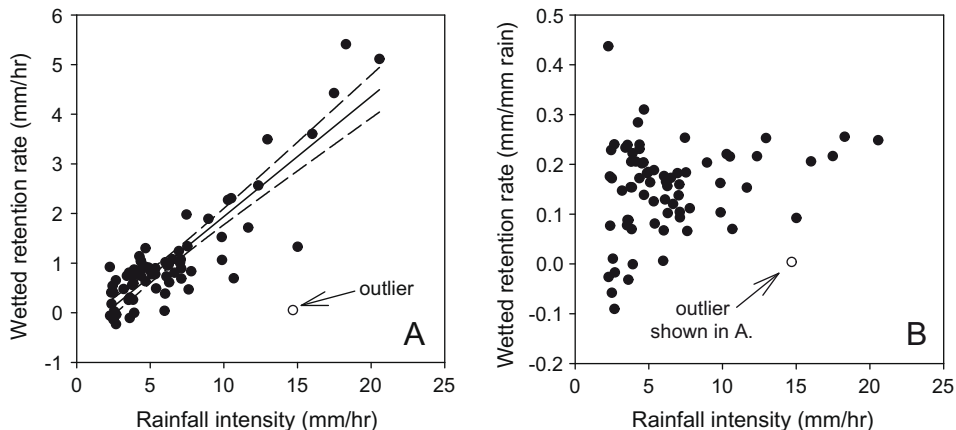
Fig. 9. Wetted retention rate (calculated as the difference between rainfall and throughfall; stemflow is thus included) during periods of uniform rainfall intensity at IVE, expressed as (A). wetted retention per unit time (dashed lines indicate 95% CI for the slope of the relation) and (B). wetted retention per millimeter of rainfall.

In a forest, the wetted surface area above the ground surface is that of the leaves, branches and stems. Leaf-area measurements near the study site suggest that one-sided leaf-area indices (projected area of leaves and green branchlets per unit ground surface area) of 13–14 are appropriate for 120-year-old redwood stands in the watershed (Kevin O'Hara, UC Berkeley, personal communication 10/21/2003). The Douglas-firs present in the stand are also expected to have high leaf-area indices, as Waring et al. (1978) found that mature Douglas-fir forests typically show values greater than 15. Measurements of cross–sections of redwood needles indicate that the cross-section perimeter is approximately 2.5 times the width of the needle, producing a total leaf-area index of about 32 to 35. If all leaf surfaces are wetted, an evaporation rate of $0.006 \, mm^3 \, h^{-1}$ per mm^2 of water surface thus would result in an actual loss of $0.21 \, mm^3 \, h^{-1}$ per mm^2 of ground surface. Measurements of bark crenulations suggest that, if fully wetted, evaporation from bark surfaces on boles and branches could account for an additional $0.01 \, mm^3 \, h^{-1}$ of evaporation per mm^2 of ground surface.

For the total leaf- and bark-area indices expected for the Caspar Creek forest, a midwinter in-rain evaporation rate of $0.21 \, mm \, h^{-1}$ would by itself be sufficient to account for about 60% of the total interception loss over the 3-year measurement period at IVE, as rain fell for 510–730 h each year. However, the full 60% would not be realized because surfaces are not fully wetted during many storms. Furthermore, interception rates observed during high-intensity rainfall (Fig. 9a) can be an order of magnitude greater than the estimated evaporation rate—an amount that would not be explained even if evaporation rates are represented by the upper bound to the 95% confidence interval ($0.42 \, mm \, h^{-1}$).

Additional mechanisms are thus required to explain the high interception rates during periods of high-intensity rainfall. In-rain evaporation in tree canopies may be higher than indicated by open-pan measurements because of exposure to wind, and the proportion of foliage surface wetted increases with rainfall intensity, contributing to an increase in evaporation with increasing intensity. In addition, small-scale turbulence increases with rain intensity, also contributing to an increase in evaporation rate per unit time with increasing rainfall intensity. Hashino et al. (2002), for example, attributes relationships such as that shown in Fig. 9a to a dependence of the aerodynamic resistance term in the Penman–Monteith equation on rainfall intensity.

The high variance exhibited in Fig. 9b would be expected if evaporation contributes significantly to in-rain interception loss: evaporation rate is ultimately controlled by atmospheric conditions, which vary between events. Open pan evaporation rates can be estimated using Penman's approach (Dunne and Leopold, 1978) as a function of temperature, wind, solar input, and vapor pressure. However, multiple regressions of interception rate against wind speed, season (a surrogate for solar input), and temperature did not further explain the variance in Fig. 9a and b, and meteorological data did not provide an explanation for the outlier shown. Vapor pressure, the remaining variable in the Penman equation, is expected to be influential but was not measured. Rain sometimes occurs while clouds—representing saturated air—are at ground level in this fog-prone area, and the outlier noted in Fig. 9 may represent such conditions. In-rain loss dropped to zero for more than an hour during 7 of the 250 events recorded at IVE and 1 of the 78 events at MUN. The increased variance and occasional negative values shown in Fig. 9 for low rainfall intensities for the most part reflect the increased relative importance of measurement uncertainties during low-intensity rainfall.

Enhanced evaporation due to shattering of drops

Additional evaporative loss could occur during high-intensity bursts because large drops are shattered and slowed by impacts with foliage. The shattered drop has a larger total surface-to-volume ratio than the intact drop and terminal velocities of the fragments are lower, allowing more efficient evaporation (Murakami, 2006). This mechanism might also contribute to the observed increase in loss rate per unit time with increasing rainfall intensity if shattering rates increase with increasing kinetic energy of the drops. However, at lower intensities the effect may be negative. Vis (1986), for example, found that coalescence of droplets on foliage can lead to an increase in the median drop diameter of throughfall relative to that of rainfall in a clearing.

The potential influence of this mechanism can be calculated if evaporation rate and droplet sizes are known. Huber et al. (1996) describe droplet size distributions for 4 mm and 5 mm drops striking 0.5-mm-thick water films; raindrops of these sizes would be expected in high-intensity rain bursts. Terminal velocity depends on drop size, which increases with intensity. Published relations (Atlas and Ulbrich, 1977) allow calculation of travel times (including reacceleration after impact) for the expected droplet sizes, and the surface area available for evaporation can be calculated from the distribution of droplet sizes. Volume evaporated is then calculated for each size class, summed, and compared to that expected for an intact drop. For a 50-m-high canopy and a $0.006 \, mm \, h^{-1}$ evaporation rate, results suggest that this effect would account for an interception loss of less than 1% during high-intensity bursts, even though the volume evaporated would increase by an order of magnitude relative to that expected for intact drops.

The evaporation rate of a falling drop is likely to be higher than that of a stationary water surface because of the high effective wind speed experienced by the falling drop. However, recalculation for a 10-fold increase in evaporation rate still produces an estimated increase in interception loss of less than 1%.

Diversion to bark storage

Redwood trees are notable for their fibrous, absorbent, deeply crevassed bark, and the high wetting threshold necessary to generate stemflow from redwoods (51 mm of rainfall) reflects the large moisture storage potential provided by bark. Comparison of dry and saturated weights of bark samples of known volume indicate that redwood and Douglas-fir bark can absorb about $0.45 \, cm^3$ and $0.15 \, cm^3$ of water per cm^3 of bark, respectively. Measurements of stem diameters, stem surface areas, and bark thicknesses provided by Steinbuck (2002) allow regression of estimated bark volumes against stem diameters for a sample of 12 redwoods and 8 Douglas-firs in the stand, and these relations can then be used to estimate total bark volume on stems of these species on the IVE plot. Results suggest that bark on conifer boles may be capable of storing the equivalent of 10–15 mm of rainfall at the site, and a variety of studies suggest that bark can indeed represent the dominant storage component in some forests (Iida et al., 2005; Crockford and Richardson, 1990a; Herwitz, 1985).

Because of the large storage potential in bark and the relatively small area contributing flow to the bole, bark will remain unsaturated under most conditions, so the bark infiltration rate is likely to be nearly constant for all but the most prolonged storms. Diversion of rainfall to bark storage would thus represent a near-constant proportion of incident rainfall for most of the monitored storms, and that proportion would depend primarily on the proportion of rainfall encountering boles and branches. The diversion rate ($mm \, h^{-1}$) to bark storage would thus appear to be proportional to rainfall intensity, in that the proportion diverted (mm stored per mm rain) would be relatively constant across the range of intensities.

The basal area of the IVE stand is $97 \, m^2 \, ha^{-1}$, so only about 1% of rainfall could encounter the bole either directly or through drip from foliage if rain is falling vertically. If wind deflects rain from vertical, potential incidence would increase substantially. A 10° deflection, for example, would result in 6% incidence. Channeling

toward the bole by up-turned branches would increase incidence still further. Steinbuck (2002) found that an average of 17% of branches on redwoods and 58% on Douglas-firs ascend from boles in the IVE stand. If each of the 146 conifers with diameters >50 cm on the IVE plot has 100 stem branches with diameters averaging 6 cm, and if the inner meter of each ascending branch contributes all incident rainfall to the stem, about 4% of rainfall would be diverted to boles. Actual values are expected to be higher due to the presence of 392 smaller trees. At a 6% incidence rate, bark storage would not reach capacity until more than 170 mm of rain has fallen. Until this point, about 6% of rainfall would be diverted to bark storage regardless of rainfall intensity. Such calculations suggest that bark storage may be an important mechanism for interception loss at the site, and further work is currently under way to quantify its influence.

Volumes of water in storage on foliage

Comparison of the time distributions of cumulative rainfall and throughfall suggests that mean residence time in dynamic foliar storage is about 10–30 min, and the duration of post-rainfall drip indicates that the maximum duration for unreplenished dynamic storage is about 3 h.

Drip at the end of an event appears as an abruptly descending segment ending the cumulative loss curve (Fig. 10), and provides an estimate of the depth of dynamic storage associated with rainfall near the end of the event. Post-storm drip for the 176 events of the first two measurement years at IVE was tabulated by time after rainfall ended at the standard rain gauge. The depth of post-storm drip for events larger than 10 mm is found to be more strongly associated with the last hour of rainfall than with rainfalls over the final 30 or 120 min. This pattern suggests that the mean residence time for water in dynamic storage can be appreciable, and a comparison of cumulative depth dripped with time after rainfall ended indeed shows that only 45% of the drip has occurred by 30 min after rainfall ends, while 71% has occurred by 60 min (Fig. 11). Overall, the average event of greater than 10 mm produced 0.3 mm of post-storm drip.

Plots of cumulative interception (calculated as the difference between cumulative rainfall and cumulative throughfall) against cumulative rainfall during an event (Fig. 7b) reveal changes in dynamic storage. Cumulative interception increases rapidly at the onset of a high-intensity rain period and then decreases when the burst ends, indicating that the drip rate is then greater than expected for the post-burst rain intensity. For a burst occurring during otherwise uniform-intensity rain, the associated increase in dynamic storage can be estimated graphically as the maximum deviation of the curve from the line connecting cumulative inter-
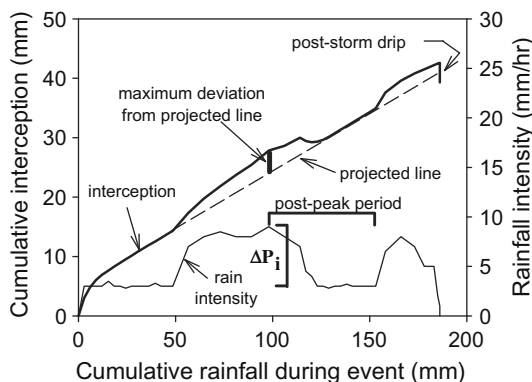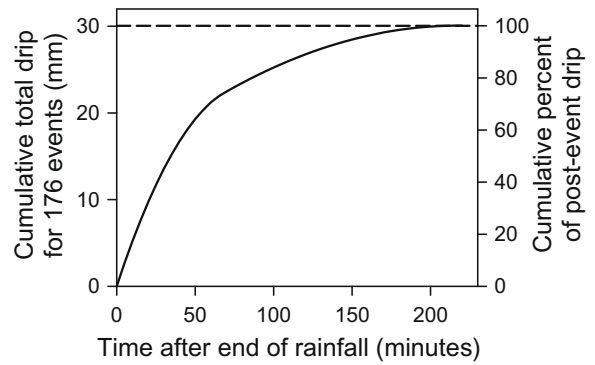

Fig. 11. Distribution through time of end-of-event drip for the first two measurement years at IVE.

ception at the beginning of the burst to that after excessive dripping has ended (Fig. 10).

During the first 2 years' record at IVE, 31 periods were identified that had relatively uniform rainfall punctuated by a high-intensity burst (selection criterion: the difference in rain intensities before and after the burst was required to be less than 25% of the maximum intensity increase during the burst). Ideally, the period of uniform intensity after the high-intensity burst would be long enough to account for most drip associated with the maximum intensity, but this is rarely the case. Actual durations of uniform post-burst rainfall varied from 20 to 165 min for these storms and averaged 37 min. The time distribution of post-storm drip (Fig. 11) was thus used to estimate, for each event, the expected proportion of drip occurring during the post-peak period (the period between the time of maximum storage and the end of the post-burst duration of uniform-intensity rain). Storage associated with the maximum rainfall intensity in each burst was then calculated using the method illustrated in Fig. 10 and divided by the estimated proportion dripped to estimate total dynamic storage for the maximum intensity increase during the burst (ΔP_i, mm h^{-1}). Estimated dynamic storage volume (S_{dm}) is found to increase as the intensity difference increases (Fig. 12):

$$S_{dm} = 0.34 + 0.092\Delta P_i \quad n = 31 \quad r^2 = 0.72 \tag{5}$$

Data from bursts followed by more than 50 min of uniform rainfall plot within the scatter of those followed by shorter periods, suggesting that errors introduced by assuming the time distribution of post-peak drip do not introduce a bias. A 10-mm h^{-1} increase in intensity thus generates an additional 1.3 mm of dynamic storage, while a 20-mm h^{-1} increase generates 2.2 mm. Background

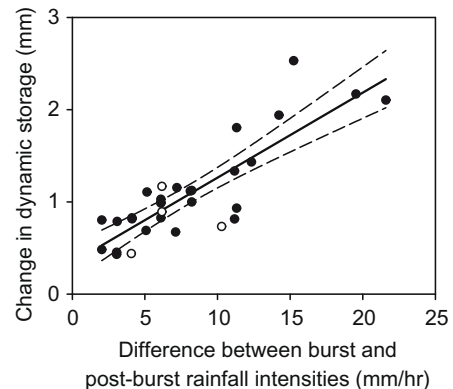Fig. 10. Increase in dynamic storage during a hypothetical high-intensity rain burst.

Fig. 12. Increase in dynamic storage as a function of increase in rainfall intensity. Dashed lines indicate the 95% confidence interval for the slope of the relation, and open symbols represent bursts followed by more than 50 min of uniform rainfall.

rain intensity does not significantly influence the result. If all surfaces are assumed to be wetted during the 20-mm h^{-1} burst and if total leaf-area index is assumed to be 35 on the basis of measured leaf cross-sections, average dynamic storage depth on the wetted surfaces would be 0.06 mm. Recalculation of values assuming that the time distribution of post-peak drip represents a twofold acceleration relative to post-storm rates reduces estimates of storage by about 35%.

Cumulative curves also allow estimation of static storage volumes on foliage. Four storms at IVE had rainfalls of over 20 mm with relatively continuous rainfall, so evaporation from static storage on leaves would have occurred only after rain ended. Subtracting the interception accounted for by wetted retention from the total interception for these storms, and using the relationship shown in Fig. 4 to estimate stemflow, produces estimated static storage of 0.63–1.5 mm with a mean of 0.97. Combining static and dynamic storage components suggests that foliar storage may exceed 3 mm during high-intensity rain bursts. Canopy storage capacities of 1–3 mm have been reported for other coniferous forests (Klaassen et al., 1998).

Influence of interception loss on the seasonal water balance

To assess the overall importance of interception loss to the Caspar Creek water balance, we first must estimate the contribution to interception by forest litter, which we did not measure. Surfaces within litter layers commonly touch others, reducing storage capacity relative to similar amounts of live foliage, and lower evaporation rates are expected because airflow is restricted. Helvey and Patric (1965) summarize studies of litter interception under hardwood forests in eastern North America and conclude that litter intercepts and evaporates about 2–5% of annual rainfall.

The seasonally distributed water balance can be estimated using a procedure based on that outlined by Dunne and Leopold (1978, p. 238). These calculations employ the average annual rainfall of 1316 mm applicable to the pre-logging period at North Fork Caspar (1963–1984), rather than the 1978–2001 average of 1285 mm, so that North Fork Caspar runoff measurements from the pre-logging period can be used in the calculations.

The 0.5- to 2-m-deep gravelly loam to clay-loam soils of the watershed's hillslopes are estimated to have available water holding capacities of about 20% (Dunne and Leopold, 1978, p. 242) and an average rooting depth of about 0.8 m (estimated from data in Wosika, 1981), producing an estimated soil moisture storage capacity of about 160 mm. A portion of the total potential evapotranspiration represents evaporation of rainfall intercepted by foliage, and this portion can now be accounted for explicitly in the calculations by applying the average loss of 25.4% (22.4% by foliage and bark and an estimated 3% by litter) to the monthly rainfall. Average interception loss for each month is first subtracted from monthly mean rainfall to estimate effective rainfall for the month, and monthly mean streamflow is then subtracted from this value to estimate the amount of water available for transpiration, soil moisture recharge, and groundwater recharge.

The method also requires an estimate of potential transpiration. Common equations for estimating evapotranspiration do not distinguish between interception and transpiration. However, the Thornthwaite equation (Dunne and Leopold, 1978) is based simply on average temperature and solar input, which are dominant controls on potential transpiration but which do not significantly influence interception at the study site. Consequently, the equation is expected to provide a useful estimate of the seasonal distribution of potential transpiration, but to overestimate the magnitude of transpiration because results of the equation implicitly include interception. The distribution of monthly potential transpiration is thus estimated using the Thornthwaite equation and the overestimate is corrected by rescaling the magnitude using the water balance calculations (Dunne and Leopold, 1978) to find an annual total potential transpiration that most closely predicts the measured mean annual runoff.

Results suggest that under conditions present before second-cycle logging at Caspar Creek, the estimated actual transpiration of 325 mm results from a potential transpiration of 394 mm. About 68% of the annual evapotranspiration occurs during October–April (Fig. 13), and during this period interception loss accounts for 67% of the evapotranspiration. Considerable uncertainty remains concerning the effects of summer fog on dry-season transpiration. Although fog drip does not appear to be an important contribution to the local water balance (Keppeler, 2007), absorption of fog water condensed on leaves may allow augmented transpiration during summer months (Burgess and Dawson, 2004).

In the past, controversy arose over whether interception loss simply compensates for suppressed transpiration during storms, since transpiration is insignificant if water blocks stomatal openings. However, studies have repeatedly demonstrated that such compensation is not large (Dunne and Leopold, 1978). Results from a pine forest suggest that the average rate of evaporation of intercepted water is three times the average transpiration rate for the same radiation level (Stewart, 1977), and measurements in a deciduous forest indicate ratios of 2.5–20 (Singh and Szeicz, 1979).

The study area has mild winters, so transpiration is expected throughout the year, but the season of lowest transpiration is that of highest rainfall and interception loss. An approximate maximum extent that reduced transpiration can offset interception at IVE can be estimated by assuming transpiration stops during rain and that night-time transpiration rates are half of day-time rates for redwoods, for which significant night-time transpiration has been documented (Burgess and Dawson, 2004). Average day- and night-time transpiration rates for each month are estimated by apportioning the estimated actual monthly transpiration over the durations of daylight and darkness for the month, given the proportional relation between day- and night-time rates. These values are then multiplied by the average durations of day- and night-time rainfall in each month to estimate suppressed transpiration. Comparison of monthly suppressed transpiration with interception loss shows that reduced transpiration can compensate for no more than 20% of interception loss. Actual compensation is likely to be less because the undersides of needles, where stomate density is highest, remain dry during some storms, and because night-time transpiration rates for species other than redwoods will remain lower than 50% of day-time rates.

Potential influences of clearcut logging

Unless a clearcut is burned, logging generally augments the litter layer with branches trimmed from boles before yarding. Foliage
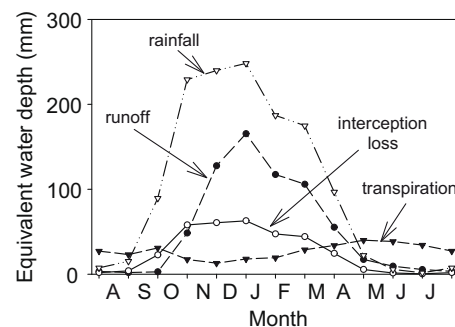

Fig. 13. Monthly water balance for forested conditions, North Fork Caspar Creek watershed.

on the ground is expected to provide lower interception rates than live foliage, but rates are expected to be higher than those for the litter layer. Kelliher et al. (1992), working in a 60% thinned and heavily pruned 7-year-old, 9-m-high *Pinus radiata* plantation in which all debris had been left in place, found that the trees (which accounted for a 1-sided leaf-area index of 1.7) intercepted 19% of annual rainfall, while logging debris (which provided a 1-sided leaf-area index of 3.5, or 67% of the total for the plot) intercepted 11%, indicating that loss rates per unit surface area of live foliage were 3.6 times those of logging debris. Estimated storage per unit surface area of debris was 40% of that for living leaves. Bark storage on 7-year-old pines is expected to be minimal.

If the proportional change in interception for cut redwood and Douglas-fir foliage is similar to that for pines and if all cut foliage is left in place, interception loss from foliar storage after logging might be estimated as 27% (1/3.6) that of the original forest, or about 6% of rainfall at Caspar Creek if bark storage is not considered. This value would decrease as foliage decays, and would be near zero if debris was burned. If interception by the original forest-floor litter is assumed to be 3% both before and after logging, effective rainfall immediately after logging would increase by a factor of 1.21, and by 1.33 if all debris and litter is burned. The change in bark storage due to removal of boles would raise the proportional increase still further.

An increase in effective rainfall during storms would contribute to increased peak flows and storm runoff after logging, and such increases would be expected throughout the storm season and even during the largest peaks. This pattern of increase contrasts with that commonly expected in rain-dominated logged areas of western North America. The widely recognized mechanisms for hydrologic change in the region are compaction and decreased transpiration after logging, so increased flows are expected only for small to moderate peaks near the beginning of the wet season (e.g., Chamberlin et al., 1991) unless compaction is severe (Harr, 1979). However, monitoring data from Caspar Creek indicate that increased peakflows after clearcutting do not conform to the expected pattern. Instead, peakflows increase throughout the season, even the largest flows are affected, and the magnitude of the increase is directly correlated to the proportion of the watershed logged (Lewis et al., 2001). This pattern is consistent with the response expected from decreased interception loss after logging.

Increased effective rainfall is also expected to increase pore pressures on hillslopes after logging, thereby potentially increasing the frequency of landsliding. Slope stability in redwood forests has often been assumed to be insensitive to logging because much of the root network persists after cutting of this stump-sprouting species; reduced root cohesion would not be as effective in generating landslides after logging as in forests of other types. However, data included in sediment source inventories from landslide-prone terrain 100 km north of the study site suggest that landsliding rates have indeed increased in some logged redwood forests in that area (e.g., PWA, 1998) despite vigorous stump-sprouting. This kind of influence might come about because of the effect of interception on short-term rain intensities, as suggested by Keim and Skaugset (2003), but an even stronger influence may well be the effective 20–30% increase in effective rainfall and antecedent wetness after logging simply due to the change in volume of rainfall intercepted.

Conclusions

Measurements of rainfall, stemflow, and throughfall at Caspar Creek indicate that approximately 22.4% of the rainfall in this 120-year-old redwood forest is stored by foliage and bark and evaporates before it reaches the litter layer. More than half of the water contributing to total interception loss is intercepted after

Table 4
Components of the mean annual watershed water balance for forested conditions, North Fork Caspar Creek watershed. Subtotals are italicized.

	equivalent water depth (mm yr^{-1})		
	Input	Transfer	Output
Rainfall (1963-1984) [a]	1316		
Throughfall to litter surface			
Free throughfall		*105*	
Delayed by foliage		*884*	
Total		989	
Stemflow		33	
Stopped by foliage and bark		293	
Interception loss			
Foliage and bark interception			*293*
Litter interception[b]			*39*
Total			332
Transpiration[c]			325
Streamflow			
Baseflow			*244*
Stormflow			*415*
Total			659
Total	1316		1316

[a] Rainfall for 1963–1976 estimated from correlation with rain gauge in the South Fork Caspar Creek watershed.
[b] Estimated to be 3% using data from Helvey and Patric (1965).
[c] Calculated as difference; may be higher than calculated due to absorption of fog water.

the initial wet-up period during a storm, either to evaporate during the storm or to be held in storage for evaporation after the storm. Because leaf-area indices are relatively high in coniferous forests, the surface area of wetted foliage is large during storms, so low evaporation rates (per unit area of water surface) can lead to large volumes of water evaporated (per unit area of ground surface). Nevertheless, interception rates observed during periods of intense rainfall appear to be too high to be explained by in rain evaporation alone, even if all foliage surfaces are wetted. An additional component of in-rain interception might be accounted for by absorption by bark. Because the water storage capacity in bark is quite large in the Caspar Creek forest, the amount of rainfall absorbed by bark during most storms is expected to be roughly proportional to the amount of rain encountering the bark. The volume of water sequestered per unit time would thus increase with rainfall intensity, while the proportion of rainfall intercepted would remain relatively constant, as observed.

Comparison of the timing of throughfall relative to rainfall in a nearby clearing indicates that the volume of water in storage in the canopy varies with rainfall intensity. Static storage in foliage is estimated to be about 1 mm, while the dynamic component of foliar storage can be as high as 2.4 mm. During periods of high-intensity rain, total foliar storage is therefore expected to exceed 3 mm.

Water balance calculations suggest that interception loss accounted for about half the annual evapotranspiration in the North Fork Caspar Creek watershed when it supported a 120-year-old redwood forest (Table 4). About 68% of the annual evapotranspiration occurs during the October–April wet season, and during this time interception accounts for about two-thirds of the loss. After clearcut logging, effective storm rainfall would have increased significantly, potentially contributing to the observed increases in post-logging peakflows at Caspar Creek.

References

Atlas, D., Ulbrich, C.W., 1977. Path and area integrated rainfall measurement by microwave attenuation in the 1–3 cm band. Journal of Applied Meteorology 16, 1322–1331.

Bryant, M.L., Bhat, S., Jacobs, J.M., 2005. Measurements and modeling of throughfall variability for five forest communities in the southeastern US. Journal of Hydrology 312, 95–108.

Burgess, S.S.O., Dawson, T.E., 2004. The contribution of fog to the water relations of *Sequoia sempervirens* (D. Don): foliar uptake and prevention of dehydration. Plant, Cell and Environment 27 (8), 1023–1034.

Chamberlin, T.W., Harr, R.D., Everest, F.H., 1991. Timber harvesting, silviculture, and watershed processes. In: Meehan, W.R., (Ed.), Influences of Forest and Rangeland Management on Salmonid Fishes and their Habitat. American Fisheries Society Special Publication 19, pp. 181–205 (Chapter 6).

Crockford, R.H., Richardson, D.P., 1990a. Partitioning of rainfall in a Eucalypt forest and pine plantation in southeastern Australia: III. Determination of the canopy storage capacity of a dry sclerophyll eucalypt forest. Hydrological Processes 4, 157–167.

Crockford, R.H., Richardson, D.P., 1990b. Partitioning of rainfall in a Eucalypt forest and pine plantation in southeastern Australia: IV. The relationship of interception and canopy storage capacity, the interception of these forests, and the effect on interception of thinning the pine plantation. Hydrological Processes 4, 169–188.

Dunne, T., Leopold, L.B., 1978. Water in Environmental Planning. San Francisco, W.H. Freeman and Co.

Gash, J.H.C., 1979. An analytical model of rainfall interception by forests. Quarterly Journal of the Royal Meteorological Society 105, 43–55.

Harr, R.D., 1979. Effects of timber harvest on streamflow in the rain-dominated portion of the Pacific Northwest. In: Proceedings of a Workshop on Scheduling Timber Harvest for Hydrologic Concerns. US Forest Service Pacific Northwest Region and Pacific Northwest Forest and Range Experiment Station, Portland, Oregon.

Hashino, M., Yao, H., Yoshida, H., 2002. Studies and evaluations on interception processes during rainfall based on a tank model. Journal of Hydrology 255, 1–11.

Helvey, J.D., Patric, J.H., 1965. Canopy and litter interception by hardwoods. Water Resources Research 1, 193–206.

Herwitz, S.R., 1985. Interception storage capacities of tropical rainforest canopy trees. Journal of Hydrology 77, 237–252.

Huber, L., Fitt, B.D.L., McCartney, H.A., 1996. The incorporation of pathogen spores into rain-splash droplets: a modelling approach. Plant Pathology 45, 506–517.

Iida, S., Tanaka, T., Sugita, M., 2005. Change of interception process due to the succession from Japanese red pine to evergreen oak. Journal of Hydrology 315, 154–166.

Keim, R.F., Skaugset, A.E., 2003. Modelling effects of forest canopies on slope stability. Hydrological Processes 17, 1457–1467.

Keim, R.F., Skaugset, A.E., Weiler, H., 2005. Temporal persistence of spatial patterns in throughfall. Journal of Hydrology 314, 263–274.

Kelliher, F.M., Whitehead, D., Pollock, D.S., 1992. Rainfall interception by trees and slash in a young *Pinus radiata* D. Don stand. Journal of Hydrology 131, 187–204.

Keppeler, E., 2007. Effects of timber harvest on fog drip and streamflow, Caspar Creek Experimental Watersheds, Mendocino County, California. In: Standiford, R.B., Giusti, G.A., Valachovic, Y., Zielinski, W.J., Furniss, M.J., (technical Eds.), Proceedings of the Redwood Region Forest Science Symposium: What does the Future Hold? General Technical Report PSW-GTR-194, US Forest Service, Pacific Southwest Research Station, Albany, CA. pp. 85–93.

Klaassen, W., Bosveld, F., de Water, E., 1998. Water storage and evaporation as constituents of rainfall interception. Journal of Hydrology 212–213, 36–50.

Lewis, J., 2003. Stemflow estimation in a redwood forest using model-based stratified random sampling. Environmetrics 14 (6), 559–571.

Lewis, J., Mori, S.R., Keppeler, E.T., Ziemer, R.R., 2001. Impacts of logging on storm peak flows, flow volumes and suspended sediment loads in Caspar Creek, California. In: Wigmosta, M.S., Burges, S.J. (Eds.), Land Use and Watersheds: Human Influence on Hydrology and Geomorphology in Urban and Forest Areas. Water Science and Application, vol. 2. American Geophysical Union, Washington, DC, pp. 85–125.

Link, T.E., Unsworth, M., Marks, D., 2004. The dynamics of rainfall interception by a seasonal temperate rainforest. Agricultural and Forest Meteorology 124, 171–191.

Liu, S., 1997. A new model for the prediction of rainfall interception in forest canopies. Ecological Modelling 99, 151–159.

Maidment, D.R. (Ed.), 1993. Handbook of Hydrology. McGraw-Hill, Inc., New York.

McMinn, R.G., 1960. Water relations and forest distribution in the Douglas-fir region on Vancouver Island. Publication 1091, Canada Department of Agriculture, Forest Biology Division, Ottawa, Canada, 71 p.

Murakami, S., 2006. A proposal for a new forest canopy interception mechanism: splash droplet evaporation. Journal of Hydrology 319, 72–82.

Patric, J.H., 1966. Rainfall interception by mature coniferous forests of southeast Alaska. Journal of Soil and Water Conservation 21 (6), 229–231.

PWA (Pacific Watershed Associates), 1998. Sediment Source Investigation and Sediment Reduction Plan for the Bear Creek Watershed, Humboldt County, California. Report Prepared for The Pacific Lumber Company. Pacific Watershed Associates, Arcata, California.

Pypker, T.G., Bond, B.J., Link, T.E., Marks, D., Unsworth, M.H., 2005. The importance of canopy structure in controlling the interception loss of rainfall: examples from a young and an old-growth Douglas-fir forest. Agricultural and Forest Meteorology 130, 113–129.

Särndal, C., Swensson, B., Wretman, J., 1992. Model Assisted Survey Sampling. Springer-Verlag, New York. 694 pp.

Singh, B., Szeicz, G., 1979. The effect of intercepted rainfall on the water balance of a hardwood forest. Water Resources Research 15 (1), 131–138.

Spittlehouse, D.L., 1998. Rainfall interception in young and mature coastal conifer forests. In: Alila, Y. (Ed.), Mountains to Sea: Human Interaction with the Hydrologic Cycle, 51st Annual Conference Proceedings; 10–12 June 1998. Canadian Water Resources Association, Victoria, BC, Canada, pp. 171–174.

Steinbuck, E., 2002. The influence of tree morphology on stemflow in a redwood region second-growth forest. M.S. Thesis, California State University, Chico, CA, 55 pp.

Stewart, J.B., 1977. Evaporation from the wet canopy of a pine forest. Water Resources Research 13 (6), 915–921.

Vis, M., 1986. Interception, drop size distributions and rainfall kinetic energy in four Colombian forest ecosystems. Earth Surface Processes and Landforms 11, 591–603.

Vrugt, J.A., Dekker, S.C., Bouten, W., 2003. Identification of rainfall interception model parameters from measurements of throughfall and forest canopy storage. Water Resources Research 39 (9), 1251. doi:10.1029/2003WR002013.

Waring, R.H., Emmingham, W.H., Gholz, H.L., Grier, C.C., 1978. Variation in maximum leaf area of coniferous forests in Oregon and its ecological significance. Forest Science 24, 131–140.

Wosika, E.P., 1981. Hydrologic properties of one major and two minor soil series of the Coast Ranges of Northern California. M.S. Thesis, Humboldt State University, Arcata, CA, 150 p.